

## Effects of synthesis conditions on existence and nonexistence of the ArF excimer laser and x-ray induced $B_2\alpha$ band in type-III fused silicas

Nobu Kuzuu

*Nippon Silica Glass Co. Ltd., Keihin Higashi-Ooi Building, 13-8, 2 Chome, Higashi-Ooi, Shinagawa-Ku, Tokyo 140, Japan*

Masataka Murahara

*Department of Electrical Engineering, Faculty of Engineering, Tokai University, 1117 Kitakaname, Hiratsuka, Kanagawa 259-12, Japan*

(Received 21 October 1994; revised manuscript received 28 February 1995)

ArF excimer laser and x-ray induced absorption bands in type-III fused silica synthesized under reducing (sample DR) and oxidizing (sample DO) conditions were investigated. Under ArF excimer laser and x-ray irradiation, an absorption band at 5.0 eV called the  $B_2\alpha$  band and ascribed to an unrelaxed oxygen-deficient center was observed only in the sample DR and was not observed in the sample DO. Emission bands at 4.4 and 2.7 eV induced by exciting the  $B_2\alpha$  band only appeared in the sample DR. The creation mechanism of the  $B_2\alpha$  band in the sample DR and the reason for the nonexistence of the  $B_2\alpha$  band in the sample DO were discussed.

### I. INTRODUCTION

Studies on radiation induced optical absorption are useful to clarify defect structures in vitreous silicas,<sup>1,2</sup> because optical absorption bands are derived not only from paramagnetic defects but also from diamagnetic defects such as oxygen-deficient centers<sup>3</sup> or dissolved molecules in glass network.<sup>4-7</sup> The nature of the radiation induced defects in vitreous silica strongly depends not only upon their type but also upon the manufacturing conditions such as atmosphere and temperature. The present authors and their co-workers studied excimer laser<sup>8-13</sup> and x-ray<sup>14,15</sup> induced absorption and emission spectra in various types of vitreous silica:<sup>16</sup> type-III fused silicas synthesized directly by flame hydrolysis of  $\text{SiCl}_4$  in a hydrogen-oxygen flame under reducing<sup>8,10,14</sup> and oxidizing<sup>9,10,14</sup> conditions, OH-free (type I) and OH-containing (type II) fused quartz made by melting of natural quartz power,<sup>11</sup> and dry and wet chemical vapor deposited (CVD) soot-remelted silicas.<sup>12,13</sup>

When studying radiation induced absorption, the following points should be noted. First, the spectrum might be a composite of more than two absorption bands even when it appears as a unique peak with no shoulder. Second, there might be absorption bands derived from different origins peaking at almost the same position.

An example of the former case is x-ray induced absorption. X-ray induced absorption spectra in type-III fused silica synthesized under reducing conditions have a peak at 5.8 eV and no shoulder, but this spectrum was fitted by five Gaussian absorption bands.<sup>15</sup>

An example of the latter case, a simple spectrum of complex origin, is the absorption bands called the  $B_2$  bands whose peaks are located near 5 eV. Tohmon *et al.*<sup>17</sup> showed that there are at least two kinds of  $B_2$  bands, named  $B_2\alpha$  and  $B_2\beta$  bands; the peak positions and full widths at half maximum (FWHM's) of the  $B_2\alpha$  band

are 5.02 and 0.35 eV, and those of the  $B_2\beta$  band are 5.15 and 0.48 eV, respectively. If such a component emerged simply by Gaussian fitting, the distinction of these two types of absorption bands by the peak position and FWHM would be difficult because the fitting process may not be unique. However, the decomposition can be made unambiguous by using photoluminescence (PL) spectra; the PL peak positions of the  $B_2\alpha$  band are 4.42 (strong) and 2.74 eV (weak), and those of the  $B_2\beta$  band are 4.24 and 3.16 eV. Kuzuu<sup>15</sup> studied x-ray induced absorption in type-III fused silica synthesized under reducing conditions containing  $(5.8-8.7)\times 10^{19}$   $\text{cm}^{-3}$  of OH, and showed that the absorption spectra having a peak at 5.8 eV and no shoulder can be constructed by five Gaussian absorption bands including a 5.0-eV band. The PL spectra showed that the 5.0-eV absorption band in these samples is the  $B_2\alpha$  band.

In Ref. 14, we compared x-ray induced absorption bands in type-III fused silicas synthesized under reducing (DR) and oxidizing (DO) conditions, and suggested the existence and nonexistence of the  $B_2\alpha$  band in samples DR and DO from the PL spectra; sample DO showed no evidence of the existence of the 5.0-eV band in the PL spectra. However, we did not try to show the existence in sample DR and nonexistence in sample DO of the  $B_2\alpha$  band by Gaussian peak decomposition.

We studied, in Ref. 8, ArF laser induced absorption and emission bands in sample DR; absorption spectra peaking at 5.8 eV and an emission band at 4.4 eV were observed. We proposed a model to describe these phenomena, and suggested a correlation between the 5.8-eV absorption and 4.4-eV emission bands in that paper. However, we could not clarify the origin of the 4.4-eV band.

In the present paper we study the origin of the ArF laser induced 4.4-eV emission band and show that this band is caused by the same defect responsible for the  $B_2\alpha$

band. Moreover, the existence of the 5.0-eV band was shown by Gaussian peak decomposition of the absorption spectra in sample DR irradiated with an ArF laser and x rays. We also confirmed by Gaussian peak decomposition that no 5.0-eV band exists in sample DO irradiated with either an ArF laser or x rays.

## II. EXPERIMENTAL PROCEDURE

### A. Samples

Type-III fused silicas synthesized directly by flame hydrolysis of  $\text{SiCl}_4$  in a hydrogen-oxygen flame under reducing (sample DR) and oxidizing (sample DO) conditions were cut from almost the same position in the same ingot as in the previous papers.<sup>8,9</sup> The OH content of samples DR and DO is  $6.2 \times 10^{19} \text{ cm}^{-3}$  (800 ppm in mass) and  $9.3 \times 10^{19} \text{ cm}^{-3}$  (1200 ppm in mass), respectively. The samples were cut into pieces of size  $10 \times 10 \times 30 \text{ mm}^3$ , and their surfaces were polished.

One of the pieces of sample DO was annealed in ambient He at  $900^\circ\text{C}$  for 2 h to accelerate creation of the ArF laser induced absorption in the same manner as in Ref. 9.

### B. Luminescence measurement

ArF excimer laser induced luminescence was measured by the same manner as in previous papers.<sup>8,9</sup> A Questek 2240 type excimer laser employing ArF as the lasing medium was utilized in the present study. The energy density was controlled by a fused silica lens ( $f = 500 \text{ mm}$ ) and the beam was adjusted to 3 mm in diameter using an iris.

The luminescence was measured from a direction perpendicular to the incident beam. Emission spectra were measured shot by shot monochromatically (using a Jasco CT-10) by a diode-array image intensifier (a Hamamatsu Photonics C2808-03). The spectral bandwidth of each measurement was about 100 nm.

### C. X-ray exposure

The x-ray exposures were accomplished utilizing the x-ray beam of a fluorescence x-ray spectrometer (a Rigaku type 3080) with a rhodium target tube operated at 50 kV and 50 mA, which are the same conditions as in previous papers.<sup>14,15</sup>

### D. Absorption measurement

X-ray induced absorption and ArF laser induced absorption in sample DO annealed in ambient He were measured by a spectrophotometer (a Shimadzu UV-3101PC). ArF laser induced absorption in sample DR was measured by an ultrasensitive spectrophotometer which is the same apparatus as in Ref. 18. The ArF laser beam was not adjusted by a lens and impinged on the center of the sample. The beam of the ultrasensitive spectrophotometer (1 cm diameter) was masked to  $5 \times 8 \text{ mm}^2$  in the measurement to measure the central portion

of the excimer laser exposed region (the area being  $22 \times 8 \text{ mm}^2$ ).

### E. Photoluminescence measurement in x-ray irradiated samples

Photoluminescence and photoluminescence excitation (PLE) spectra in the samples irradiated with x rays for 3 h were measured by a fluorescence spectrophotometer (a Jasco FP-770).

## III. RESULTS

### A. ArF-laser induced luminescence

Examples of emission spectra of samples DR and DO are shown in Fig. 1. Figure 2 shows the shot-number dependence of ArF laser induced emission spectra near 4 eV. In sample DR, a luminescence peak at 4.1 eV appeared in a short irradiation time. With increasing shot number, the 4.1-eV peak disappeared and an emission band at 4.4 eV increased with increasing shot number. A similar luminescence peaking at 4.1 eV as appeared in short irradiation time in sample DR also appeared in sample DO and decreased with increasing shot number, but the 4.4-eV band did not appear. The peak position and the FWHM of the 4.4-eV band in Fig. 1 are 4.43 and 0.48 eV, respectively.

In addition to the 4.4-eV band, a weak emission band at 2.7 eV was induced in sample DR as shown in Fig. 3. As in the case near 4 eV, broad luminescence appeared at low shot numbers in both samples and decreased with increasing irradiation time. After sufficiently high irradiation times such broad luminescence disappeared and an absorption band at 2.7 eV appeared.

### B. ArF laser induced absorption bands

As shown in Fig. 4, the absorption spectrum in sample DR irradiated with the ArF laser measured by an ultrasensitive spectrophotometer can be decomposed into five Gaussian peaks at 6.5, 5.8, 5.4, 5.0, and 4.8 eV. The peak positions and FWHM's shown in Table I are con-

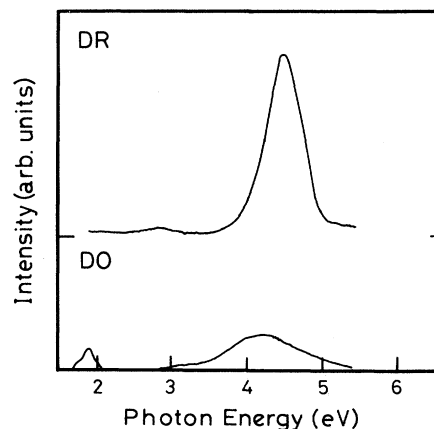


FIG. 1. Luminescence spectra of samples DR and DO irradiated with an ArF excimer laser ( $200 \text{ mJ/cm}^2$ , 100 Hz,  $6.0 \times 10^3$  shots).

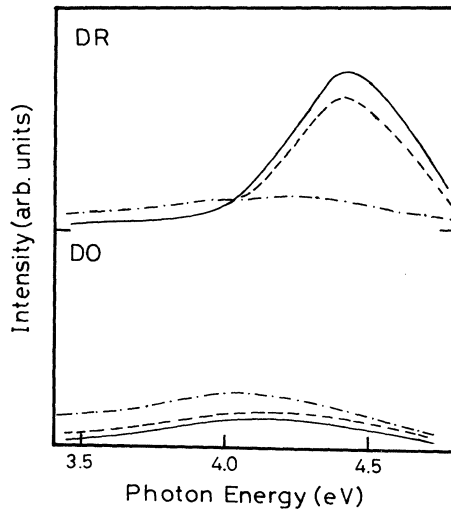


FIG. 2. Shot-number dependence of luminescence spectra of samples DR and DO near 4 eV irradiated with an excimer laser (200 mJ/cm<sup>2</sup>, 100 Hz): Solid curve,  $6.0 \times 10^3$  shots, dashed curve,  $3.0 \times 10^3$  shots, and dashed-and-dotted curve  $1.0 \times 10^2$  shots. The peak position and FWHM of the sample DR irradiated with  $6.0 \times 10^3$  shots are 4.43 and 0.48 eV, respectively.

strained to be the same as those derived in Ref. 15 for the case of x rays.

In sample DO, we also measured an ArF laser induced absorption spectrum by the ultrasensitive spectrophotometer. However, peak decomposition to sufficient accuracy was difficult because the absorption is very weak, and scatter is observed in the value of data obtained. Thus, in place of the as-manufactured sample, a sample heat treated in ambient He was used as in the case of Ref. 9; the sample shows strong absorption after irradiating with the ArF laser as shown in Fig. 5. The absorption components could be fitted by Gaussian absorption bands with the same values of peak positions and FWHM's as in the case of the sample DR. However, the best-fit result is obtained by fitting only four absorption bands, excluding the 5.0-eV band. In addition to these absorption bands, a weak absorption band at 2.0 eV was observed as in the case of Ref. 9.

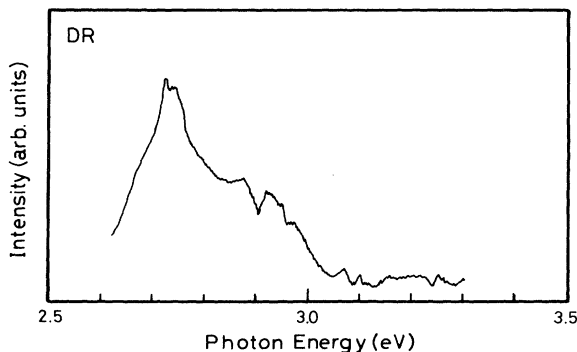


FIG. 3. ArF laser (200 mJ/cm<sup>2</sup>, 100 Hz,  $6.0 \times 10^3$  shots) induced luminescence spectra near 3 eV in sample DR.

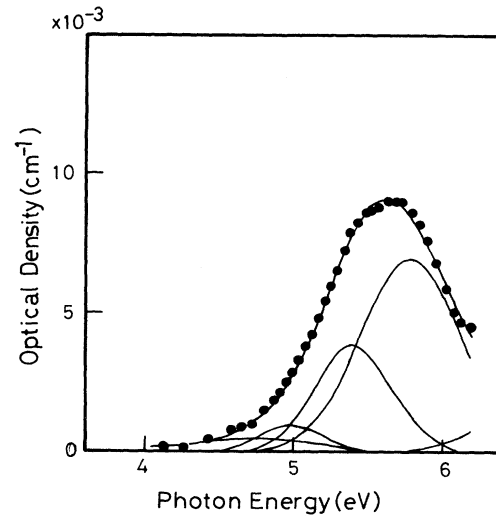


FIG. 4. ArF laser (50 mJ/cm<sup>2</sup>, 100 Hz,  $6.0 \times 10^4$  shots) induced absorption spectra in sample DR measured by an ultrasensitive spectrometer.

### C. X-ray induced absorption

The x-ray induced absorption spectrum in sample DR shown in Fig. 6(a) also could be fitted by five Gaussian peaks, at 6.5, 5.8, 5.4, 5.0, and 4.8 eV, as in the case of ArF laser irradiation. The values of the peak positions and FWHM's obtained by least-squares fits are shown in Table I.

The x-ray induced absorption in sample DO shown in Fig. 6(b) can also be decomposed into absorption bands at 6.5, 5.8, 5.4, and 4.8 eV as in the case of ArF laser irradiation (Fig. 5) and the 5.0-eV band does not appear either. In this case we used an as-manufactured sample as in the case of Ref. 14. It is noted that the relative intensity of the 5.8-eV band is higher than in the case of ArF laser irradiation; the ArF laser induced absorption spec-

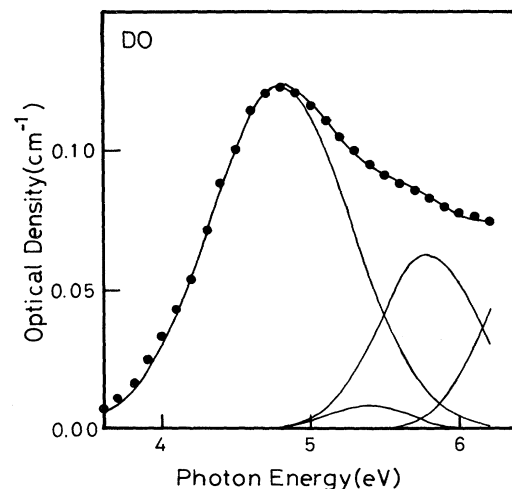


FIG. 5. ArF laser (200 mJ/cm<sup>2</sup>, 100 Hz,  $6.0 \times 10^4$  shots) induced absorption spectra in sample DO annealed in ambient He.

TABLE I. Peak positions and FWHM's of absorption components.

Band (eV)	ArF laser irradiation				X-ray irradiation			
	Sample DR		Sample DO		Sample DR		Sample DO	
	Peak	FWHM	Peak	FWHM	Peak	FWHM	Peak	FWHM
6.5	6.50	0.74	6.50	0.74	6.50	0.66	6.50	0.89
5.8	5.79	0.80	5.79	0.80	5.79	0.82	5.79	0.85
5.4	5.41	0.61	5.41	0.61	5.40	0.62	5.38	0.60
5.0	4.99	0.51			5.02	0.38		
4.8	4.79	1.12	4.79	1.12	4.76	0.96	4.78	1.15

tra shown in Fig. 5 have a peak at 4.8 eV and no shoulder, whereas the x-ray induced absorption spectra have a peak at 5.8 eV and a shoulder at 4.8 eV. In addition to these bands, weak absorption bands at 2.0 eV were observed as in the case of Ref. 14.

The values of peak positions and FWHM's agree fairly well with each other in the case of ArF and x-ray irradiated samples as shown in Table I; they indicate the reliability of the peak decomposition. Although the FWHM of the 4.8-eV band in the x-ray irradiated sample DR is a little smaller than in the case of the laser irradiated sample DR, this could be derived from numerical error be-

cause the relative intensity of this band is considerably smaller.

Figure 7 shows the x-ray irradiation time dependence of the absorption components of samples DR (a) and DO (b). In sample DR, the peak value of the absorption spectrum is almost the same as the intensity of the 5.8 eV band. In the sample DO, the growth curves of these four components have the same slope in a doubly logarithmic plot.

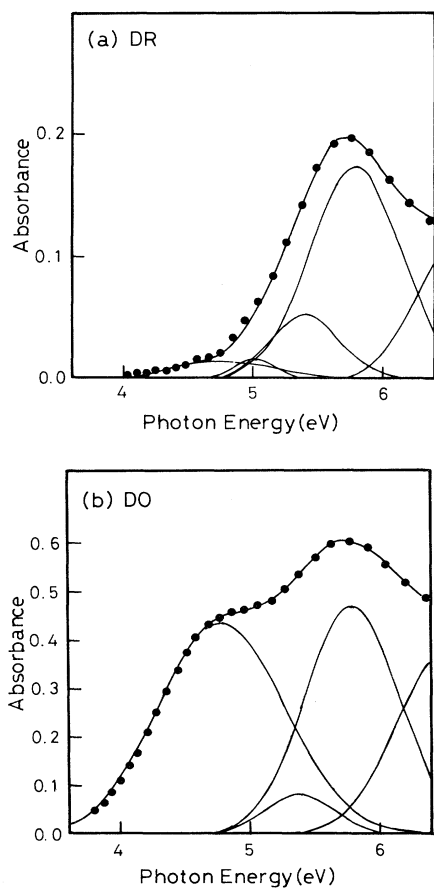


FIG. 6. X-ray induced absorption spectra in (a) sample DR and (b) sample DO. X rays from a rhodium target were operated at 50 kV and 50 mA and exposed for 3 h.

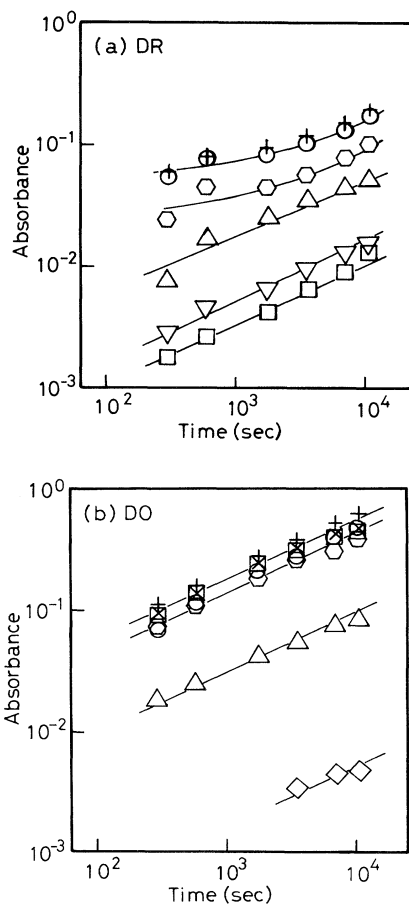


FIG. 7. Irradiation time dependence of the x-ray induced absorption components in samples (a) DR and (b) DO. (○: 5.8 eV, Δ: 5.4 eV, ▽: 5.0 eV, □: 4.8 eV, ◇: 2.0 eV, ○: 6.5 eV, +: absorption intensities at 5.8 eV, and ×: absorption intensities at 4.8 eV.)

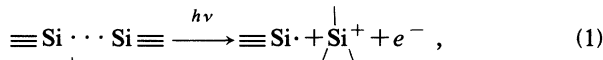
## IV. DISCUSSION

## A. Origin of 4.4-eV emission band in sample DR

As shown in Fig. 2, the 4.4-eV emission band in sample DR grows with increasing shot number of the ArF laser pulses. The peak position and FWHM of the 4.4-eV band are 4.43 and 0.48 eV, respectively. Combined with the 4.4-eV band, a very weak luminescence peak at 2.7 eV (peak intensities are about one-thirtieth of the 4.4-eV band) is created. Such luminescence is characteristic of the  $B_2\alpha$  band; the reported value<sup>17</sup> of the peak position is 4.42 eV which is equal to the ArF laser induced 4.4-eV band within the experimental error. To compare the FWHM in the  $B_2\alpha$  band, we measured the PL spectra of a soot-remelted silica having a strong  $B_2\alpha$  band (see Ref. 14); the peak position and FWHM of the PL band are 4.37 and 0.46 eV, respectively, which are comparable to those of the ArF laser induced 4.4-eV band (4.43 and 0.48 eV, respectively). In addition to the correspondence of the peak position and FWHM of the 4.4-eV band, the existence of the 2.7-eV band supports the postulate that the ArF laser induced 4.4-eV band is derived from the  $B_2\alpha$  band. The ArF laser induced emission band in a soot-remelted silica having the  $B_2\alpha$  band also shows an emission band at 2.7 eV in addition to the 4.4-eV band.<sup>19</sup>

Further evidence of the existence of the  $B_2\alpha$  band is the 5.0-eV absorption band emerging from the peak decomposition of the absorption spectra shown in Fig. 4.

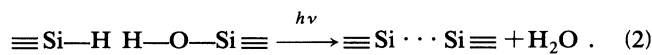
The assignment of the absorption components has been described in a previous paper.<sup>15</sup> The 5.8-eV band is a kind of  $E'$  center ( $\equiv\text{Si}\cdot$ ) called the  $E'_\gamma$  center caused by<sup>1</sup> the reaction



in which  $\overset{\text{O}}{\underset{\text{O}}{\text{Si}}}\text{O}$  represents a planar three-oxygen coordinated structure and  $\equiv\text{Si}\cdots\text{Si}\equiv$  represents an unrelaxed oxygen-deficient center (ODC) causing the  $B_2\alpha$  band. The 5.4-eV band is also a kind of  $E'$  center called the  $E'_\beta$  center which is related to hydrogen.<sup>1</sup> The 4.8-eV band is an oxygen-related center and some models have been proposed:<sup>1</sup> dissolved oxygen,<sup>4</sup> nonbridging oxygen hole centers ( $\equiv\text{Si}-\text{O}\cdot$ ),<sup>20</sup> and peroxy radicals ( $\equiv\text{Si}-\text{O}-\text{O}\cdot$ ).<sup>21</sup>

The 5.0-eV band component in the x-ray irradiated sample DR [Fig. 6(a)] is also derived from the  $B_2\alpha$  band, which is shown by the PL and PLE spectra shown in Fig. 8; a PL peak at 4.3 eV and a weak emission band at 2.7 eV were observed by exciting with 5.0-eV photons.

A probable mechanism to produce the ODC is as described in Ref. 15 in the case of x-ray irradiation: the precursor is the  $\equiv\text{Si}-\text{H}\text{H}-\text{O}-\text{Si}\equiv$  structure and is produced by the reaction



Most ODC's in the right-hand side of Eq. (2) will be changed into the  $E'_\gamma$  center by Eq. (1).

It might be considered that the ODC is created by breaking Si—O—Si bonds by the reaction

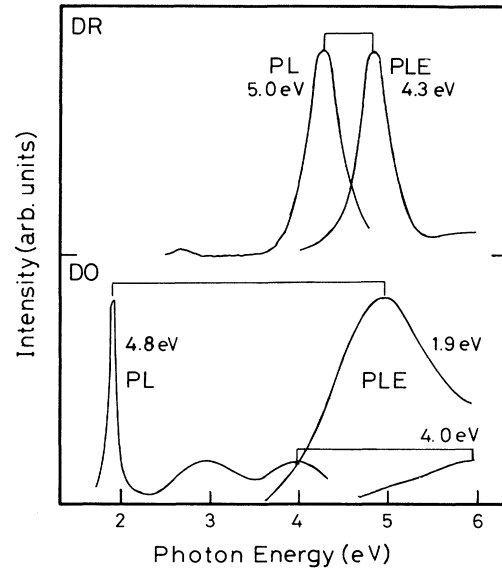
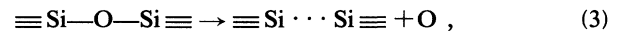


FIG. 8. Photoluminescence and photoluminescence excitation spectra in both samples irradiated with x rays for 3 h.



which can explain the existence of ODC's and  $E'_\gamma$  centers by successive production of the ODC and then the  $E'_\gamma$  center by the reaction of Eq. (1). However, this mechanism cannot explain the effect of preirradiation annealing on the creation of the 4.4-eV band described in Ref. 8. Therefore the mechanism described by Eq. (3) is not the main process at least in the case of ArF excimer laser irradiation.

Matsumoto, Yoshikado, and Murahara<sup>22</sup> studied the excimer laser induced absorption and emission bands in a sample similar to DR. The ArF laser light (6.4 eV) was first directed into the sample, which was then exposed to KrF laser light (5.0 eV) directly after cessation of the ArF laser irradiation. When irradiated with the ArF laser, the intensity of the 4.4-eV band increases with increasing shot number as in the case of the sample DR, whereas the intensity decreases with increasing shot number of the KrF laser. By ArF laser irradiation, absorption spectra peaking at 5.8 eV are induced. By the subsequent irradiation of the KrF laser, absorption intensities around 5.0 eV are decreased with increasing shot number. These phenomena can be explained as follows. Growth of the 4.4-eV band by ArF laser irradiation can be caused by the reaction of Eq. (2). Successive decrease by the KrF laser irradiation can be caused by the reaction of Eq. (1) because the KrF laser photon (5.0 eV) directly excites the ODC.

Probable creation mechanisms of the other absorption components in samples DR and DO are described in Ref. 15. Since the purpose of the present paper is to describe the creation mechanism of the 4.4-eV emission band, we do not review them here.

### B. Nonexistence of the $B_2\alpha$ band in sample DO

In the ArF excimer laser and the x-ray irradiated sample DO, the 5.0-eV band does not appear in the Gaussian peak decomposition as shown in Figs. 5 and 6(b). If we try to fit the absorption spectrum by least squares, assuming five Gaussian components as in the case of the sample DR, the peak intensity of the 5.0-eV band has a negative value, and the fitted curve is worse than in the case of four Gaussian components.

The nonexistence of the  $B_2\alpha$  band in sample DO is also supported by the PL and PLE spectra in the x-ray irradiated sample shown in Fig. 8; a strong PL peak at 1.9 eV excited by 4.8-eV photons and a broad PLE band at 4.8 eV were observed. When excited by 5.0-eV photons, broad peaks at 4.0 and 2.8 eV were also observed. However, when we monitored the PLE spectra at 4.0 eV, tails from a peak at higher photon energy than 5.9 eV were observed. Although we cannot completely exclude the possibility of the existence of the 5.0-eV PLE band with these data, it must be very weak if it exists at all.

In Ref. 14 we proposed a model to describe the x-ray induced 5.8- and 4.8-eV absorption bands. In that model, there is no mechanism to produce ODC's. In the case of x-ray irradiation, the ODC might be created by bond breakage, but it could react with oxygen or hydrogen atoms produced by photo-decomposition.<sup>15</sup> Thus ODC's produced by bond breakage would be destroyed as rapidly as they are created.

It should be noted that the relative intensity of the 5.8-eV band to the 4.8-eV band in the x-ray induced absorption is almost three times greater than that in the case of the ArF laser induced absorption. One probable reason, as discussed in Ref. 14, is the creation of the  $E'$  center from a preexisting precursor, which is strongly promoted by irradiating with x rays, because of the long irradiation times and high photon energy. Another probable reason, as pointed out in Ref. 15, is that bond breakage can only occur in the case of x-ray irradiation.

### C. Irradiation time dependence of the absorption components

We also compared the irradiation time dependence of the intensities of the x-ray induced absorption components as in Ref. 15. Figure 7 shows the irradiation

time dependence of the absorption components in samples DO and DR.

In the sample DO, the slopes of the four absorption components are 0.5 in a doubly logarithmic plot. In sample DR the time dependencies of absorption components are similar to those in Ref. 15; the intensities of the 6.5- and 5.8-eV bands are concave upward and the slopes of the irradiation time dependences of the 5.4-, 5.0- and 4.8-eV bands are 0.5 in a doubly logarithmic plot. However, the order of the 4.8- and 5.0-eV bands is opposite to that in the previous paper.<sup>15</sup>

Since the 4.8-eV band is related to the stoichiometrically excess amount of oxygen in the silica, it strongly depends on the history of the production conditions. Thus the order of the intensities of the 5.0- and 4.8-eV bands is interchangeable by subtle changes in production conditions.

## V. SUMMARY AND CONCLUSION

ArF laser and x-ray induced absorption bands in type-III fused silicas synthesized under reducing and oxidizing conditions were investigated. A fused silica synthesized under reducing conditions shows emission bands at 4.4 eV and a weak peak at 2.7 eV, which are due to the same defect giving rise to an absorption band at 5.0 eV called the  $B_2\alpha$  band ascribed to an unrelaxed oxygen-deficient center. The existence of the 5.0-eV band was supported by a Gaussian peak decomposition of the absorption spectra. By peak decomposition, absorption bands at 5.8, 5.4, and 4.8 eV are also observed. Similar absorption bands are also observed in an x-ray irradiated sample.

In a fused silica synthesized under oxidizing conditions, no such ODC exists in either ArF laser or x-ray irradiated samples because no evidence of the existence of the  $B_2\alpha$  band was observed; neither PL bands at 4.4 and 2.7 eV nor the absorption band at 5.0 eV were observed. This is because no precursors of the ODC exist in the oxidized samples and none are created in the case of ArF laser irradiation. In the case of x-ray irradiation, ODC's could be induced by bond breakage, but they could react with oxygen or hydrogen atoms produced by photo-decomposition and hence would be destroyed as rapidly as they are created.

<sup>1</sup>D. L. Griscom, J. Ceram. Soc. Jpn. **99**, 923 (1991).

<sup>2</sup>D. L. Griscom, J. Non-Cryst. Solids **73**, 51 (1985).

<sup>3</sup>H. Imai, K. Arai, H. Imagawa, H. Hosono, and Y. Abe, Phys. Rev. B **38**, 12 772 (1988).

<sup>4</sup>K. Awazu and H. Kawazoe, J. Appl. Phys. **65**, 3584 (1990).

<sup>5</sup>K. Awazu, Bunko Kenkyu **41**, 81 (1992).

<sup>6</sup>K. Awazu, H. Kawazoe, K. Muta, T. Ibuki, K. Tabayashi, and K. Shobatake, J. Appl. Phys. **69**, 1849 (1991).

<sup>7</sup>K. Awazu, H. Kawazoe, and K. Muta, J. Appl. Phys. **69**, 4183 (1991).

<sup>8</sup>N. Kuzuu, Y. Komatsu, and M. Murahara, Phys. Rev. B **44**, 9265 (1991).

<sup>9</sup>N. Kuzuu, Y. Komatsu, and M. Murahara, Phys. Rev. B **45**, 2050 (1992).

<sup>10</sup>N. Kuzuu, Y. Komatsu, and M. Murahara, Phys. Rev. B **47**,

3078 (1993).

<sup>11</sup>N. Kuzuu and M. Murahara, Phys. Rev. B **47**, 3083 (1993).

<sup>12</sup>N. Kuzuu, Y. Matsumoto, and M. Murahara, Phys. Rev. B **48**, 6952 (1993).

<sup>13</sup>N. Kuzuu, Y. Matsumoto, and M. Murahara, in *Optical Waveguide Materials*, edited by M. M. Broer, H. Kawazoe, G. H. Sigel, and R. Th. Kersten, MRS Symposia Proceedings No. 244 (Materials Research Society, Pittsburgh, 1992), p. 33.

<sup>14</sup>N. Kuzuu and M. Murahara, Phys. Rev. B **46**, 14 486 (1992).

<sup>15</sup>N. Kuzuu, J. Non-Cryst. Solids **179**, 170 (1994).

<sup>16</sup>A. Hayashi, New Ceramics **2**, 9 (1989).

<sup>17</sup>R. Tohmon, M. Mizuno, Y. Ohki, K. Sasegawa, and Y. Hama, Phys. Rev. B **39**, 1337 (1989).

<sup>18</sup>Y. Nakamura, H. Yamashita, T. Fukunishi, M. Shigeoka, F. Asakawa, and J. Ohfuku, J. Non-Cryst. Solids **105**, 114

- (1988).
- <sup>19</sup>Y. Matsumoto, N. Kuzuu, and M. Murahara, in *Optical Waveguide Materials* (Ref. 13), p. 27.
- <sup>20</sup>L. N. Skuja and A. R. Silin, *Phys. Status Solidi A* **56**, K11 (1979).
- <sup>21</sup>H. Hosono and R. A. Weeks, *J. Non-Cryst. Solids* **116**, 289 (1990).
- <sup>22</sup>Y. Matsumoto, Y. Yoshikado, and M. Murahara, in *Beam-Solid Interactions: Fundamentals and Applications*, edited by M. A. Nastasi, L. R. Harriott, N. Herbots, and R. S. Averback, MRS Symposia Proceedings No. 279 (Materials Research Society, Pittsburgh, 1993), p. 723.